A mechanistic model for permeability evolution in fractured sorbing media

Shugang Wang,[1] Derek Elsworth,[1] and Jishan Liu[2]

Received 7 September 2011; revised 27 April 2012; accepted 30 April 2012; published 14 June 2012.

[1] A mechanistic model is presented to represent the evolution of permeability in fractured sorbing media such as coal beds and organic-rich shales. This model accommodates key competing processes of poromechanical dilation and sorption-induced swelling. We show that the significant difference in stiffness between fracture and matrix transforms the composite system from globally unconstrained to locally constrained by the development of a virtual "stiff shell" that envelops the perimeter of a representative elementary volume containing a fracture. It is this transformation that results in swelling-induced permeability reduction at low (sorbing) gas pressures and self consistently allows competitive dilation of the fracture as gas pressures are increased. Importantly, net dilation is shown to require a mismatch in the Biot coefficients of fracture and matrix with the coefficient for the fracture exceeding that for the matrix—a condition that is logically met. Permeability evolution is cast in terms of series and parallel models with the series model better replicating observational data. The model may be cast in terms of nondimensional parameters representing sorptive and poromechanical effects and modulated by the sensitivity of the fracture network to dilation or compaction of the individual fractures. This latter parameter encapsulates the effects of fracture spacing and initial permeability and scale changes in permeability driven by either sorption or poromechanical effects. This model is applied to well-controlled observational data for different ranks of coals and different gases (He, CO_2) and satisfactory agreement is obtained.

Citation: Wang, S., D. Elsworth, and J. Liu (2012), A mechanistic model for permeability evolution in fractured sorbing media, *J. Geophys. Res.*, *117*, B06205, doi:10.1029/2011JB008855.

1. Introduction

[2] Gas flow and transport in fractured coals and organic-rich shales is relevant to a broad variety of scientific and industrial problems and processes (e.g., carbon geological sequestration, coalbed methane and organic-rich shale gas production, stability of coal seams). The evolution of transport characteristics in these media is controlled by competition between the mechanical and chemical effects that either generate or destroy connected porosity. These effects are especially important in fractured coals and organic-rich shales, where both permeability and stiffness are intrinsically controlled by the most hydraulically conductive, and most mechanically soft, elements, viz. the fractures. A schematic depiction of gas migration in coal seams at a variety of scales is illustrated in Figure 1. Although the feedbacks between the evolution of permeability and such processes as poromechanical response, gas sorption/desorption, and coal swelling/shrinkage have been quantitatively explored under a variety of boundary conditions both in the laboratory [*Chen et al.*, 2010, 2011; *Cui and Bustin*, 2005; *Harpalani and Chen*, 1997; *Harpalani and Schraufnagel*, 1990; *Izadi et al.*, 2011; *Liu and Rutqvist*, 2010; *Liu et al.*, 2011a, 2011b, 2011c; *Mazumder and Wolf*, 2008; *Pan et al.*, 2010; *Pini et al.*, 2009; *Robertson and Christiansen*, 2007; *Seidle and Huitt*, 1995; *Siriwardane et al.*, 2009; *Wang et al.*, 2011], and in situ [*Fujioka et al.*, 2010; *Gierhart et al.*, 2007; *Palmer*, 2009; *Palmer and Mansoori*, 1996; *Palmer et al.*, 2006; *Shi and Durucan*, 2005] significant challenges remain. Permeability can be altered spatially and temporally with different patterns and rates. The mechanisms underlying these responses are not fully understood and thus it is difficult to predict the response to mechanical stress and pore pressure perturbations, each of which may induce substantial changes in permeability.

[3] A variety of permeability models have been developed to represent the complexity of the multiple physical and chemical processes involved in gas transport in fractured sorbing media [*Connell et al.*, 2010; *Cui and Bustin*, 2005; *Izadi et al.*, 2011; *Liu and Rutqvist*, 2010; *Liu et al.*, 2011a, 2011b, 2011c; *Palmer and Mansoori*, 1996; *Robertson and*

[1]Department of Energy and Mineral Engineering, EMS Energy Institute, and G^3 Center, Pennsylvania State University, University Park, Pennsylvania, USA.
[2]School of Mechanical and Chemical Engineering, University of Western Australia, Crawley, Western Australia, Australia.

Corresponding author: S. Wang, Department of Energy and Mineral Engineering, EMS Energy Institute, and G^3 Center, Pennsylvania State University, 230 Hosler Bldg., University Park, PA 16802, USA. (szw138@psu.edu)

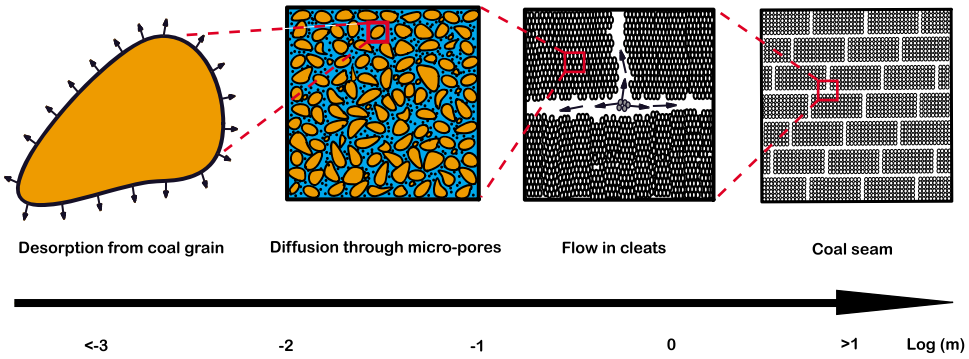

Figure 1. Schematic of gas migration in coal seams at a variety of scales.

Christiansen, 2007; *Seidle and Huitt*, 1995; *Shi and Durucan*, 2005; *Zhang et al.*, 2008]. These are summarized systematically in Appendix A and critically reviewed by *Liu et al.* [2011b] for the mostly commonly used existing models. These models are either expressed in an exponential form or in a parallel-coupled cubic form, as described in equations (1) and (2)

$$\frac{k}{k_0} = \exp(A - B), \tag{1}$$

$$\frac{k}{k_0} = (1 + A - B)^3, \tag{2}$$

where A represents poromechanical effects on the permeability, and B represents the effects of matrix swelling/shrinkage on the permeability. The validity of the cubic law for laminar flow of fluids through open and closed fractures has been established [*Witherspoon et al.*, 1980]. Numerous researchers have used the cubic law to develop permeability models that can match the experimental results on coal reasonably well [e.g., *Liu and Rutqvist*, 2010; *Pan and Connell*, 2012; *Robertson and Christiansen*, 2007]. The cubic law is derived under the assumption that the fracture consists of a region bounded by two smooth parallel plates. A natural fracture clearly deviates from a pair of smooth parallel plates in several ways, including roughness and variable apertures. Fracture aperture is the dominant factor controlling the magnitude of permeability, thus the determination of the mean aperture is crucial. *Witherspoon et al.* [1980] shows that the cubic law holds regardless of the loading path and no matter how often the loading process is repeated. Since the proposed permeability model in this study is based on the cubic law, any change in fracture aperture due to the poromechanical response or swelling response is critical in determining the net permeability change. The accuracy of the fracture aperture is the uncertainty of the model. Despite some of its limitations and assumptions, the cubic law is still the fundamental concept for understanding flow in fractures [*Zimmerman and Bodvarsson*, 1996].

[4] Under constant total stress boundary conditions, with increasing pore pressure, one would expect permeability to monotonically increase since sorption-induced swelling (free expansion) does not influence fracture aperture and fracture permeability [*Connell et al.*, 2010; *Izadi et al.*, 2011; *Liu et al.*, 2011c]. However, this is not consistent with laboratory observations [*Harpalani and Chen*, 1997; *Mazumder and Wolf*, 2008; *Pan et al.*, 2010; *Pini et al.*, 2009; *Wang et al.*, 2011] which show a dramatic initial reduction in permeability with increasing pressure of the sorbing gas. This discrepancy between observation and theory is believed to be due mainly to the heterogeneous sorption and swelling, specifically, the interaction between fractures and matrix [*Izadi et al.*, 2011; *Liu and Rutqvist*, 2010; *Liu et al.*, 2011a; *Wang et al.*, 2011]. The crucial role of this interaction is the focus of new attempts to explain this conceptual inadequacy. *Liu and Rutqvist* [2010] propose an internal swelling stress concept suggesting that only a portion of swelling strain contributes to the change in permeability. *Liu et al.* [2011a] and *Wang et al.* [2011] elucidate this mismatch by considering that the role of swelling strains is accommodated both over contact bridges that hold cleat faces apart and over the noncontacting span between these bridges. A mechanistic model proposed by *Izadi et al.* [2011] has demonstrated the important role of coal matrix-fracture compartment interactions on the evolution of coal permeability.

[5] Laboratory experimental data show that for the same type of coal sample under the same total stress and pore pressure conditions, different fracture geometries produce different permeability evolution patterns [*Wang et al.*, 2011]. Specifically, permeability reduces first with increasing pore pressure and then rebounds for ubiquitously fractured coal under constant total stress conditions. However, this regime of decreasing permeability in the swelling regime is not observed for a fully cleaved fracture in coal absent joining rock bridges. This observation implies that the presence of bridges across fractures is a crucial component in controlling the permeability evolution with pore pressure. Indeed, the important interaction between matrix and fracture has been recognized in controlling the evolution of transport constitutive relations for fractured coals. These interactions are especially important in fractured rocks, where both mechanical stiffness and permeability, are sensitive to small changes in fracture aperture. Despite this importance, very little is known about this interaction, especially quantitatively.

[6] To understand the important interaction between fracture and matrix, we explore the changes in fracture aperture that result when a fracture is subjected to an increasing pore pressure while total stress is kept constant.

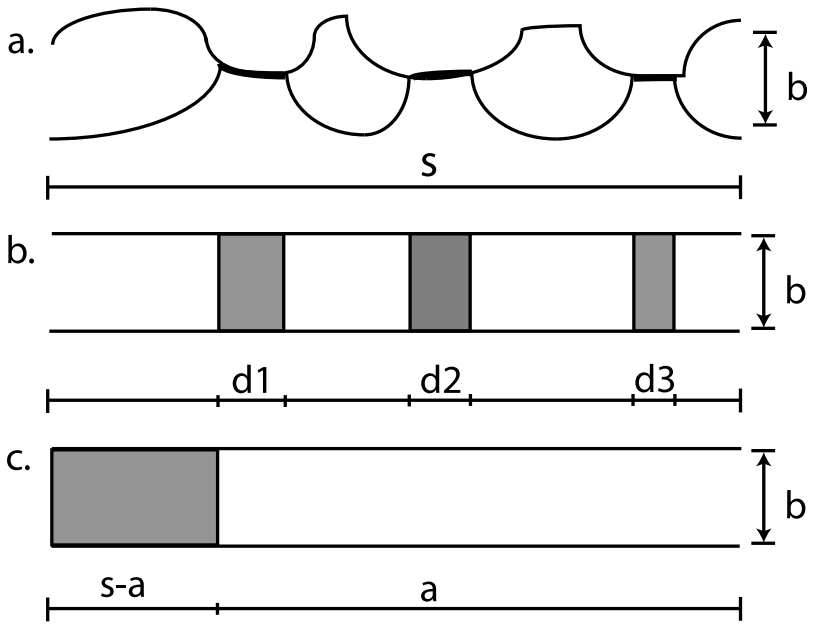

Figure 2. (a) Section view of a fracture, (b) fracture with parallel surfaces and isolated asperities, and (c) idealized asperities and void spaces. The aperture is b and the characteristic asperity dimension is s-a [after *Zimmerman et al.*, 1992].

The processes involve fracture aperture opening due to reduction in effective stress, and homogenized fracture aperture closure due to gas sorption-induced matrix volumetric swelling. We derive a cubic permeability model that can replicate these processes for permeability evolution in fractured sorbing media. We discuss the potential difference in permeability by evaluating both the parallel and series models. We find the series-coupled cubic form honors our observations recovered from carefully constrained laboratory experiments on coal samples [*Wang et al.*, 2011]. This model accommodates gas sorption-induced swelling and poromechanical response while explicitly accommodating the mechanical characteristics of the dual stiffness fracture-matrix system.

[7] In the following we present a conceptual model of permeability evolution in coal due to concurrently overprinted sorption-induced swelling and poromechanical responses. We then validate this model using our experimental results. Finally, we discuss possible applications of the results to field conditions applicable to carbon sequestration and coalbed methane extraction.

2. Mechanistic Model

[8] Heterogeneous porous media containing two distinct forms of porosity (fracture and matrix) may be idealized as a dual porosity medium as represented by *Warren and Root* [1963]. In these rock masses, both mechanical and hydraulic behavior is controlled by the presence of fractures. Fracture stiffness and fluid flow through a single fracture under normal stress are implicitly related to the geometry of the fracture and contact areas that compose the fracture [*Pyrak-Nolte and Morris*, 2000]. A typical fracture contains isolated asperity regions where the two surfaces are in contact, surrounded by open regions where the two surfaces are separated by an aperture b that may vary from point to point, as illustrated in Figure 2a. When fluid flows through such a fracture, it flows around the contact areas, but also has a tendency to flow preferentially through the channels with the largest apertures, as hydraulic conductance is proportional to b^3 [*Elsworth and Goodman*, 1986; *Piggott and Elsworth*, 1993; *Zimmerman et al.*, 1992]. In this paper, we consider idealized fractures consisting of two parallel surfaces, with isolated regions of contact, as shown in Figure 2b. These contact areas have the effect of decreasing the permeability and limiting the deformation of the fracture. Neglecting turbulent flow and assuming only flow within the fracture system, the initial permeability k_0 of a set of parallel fracture of spacing, s, can be defined as [*Bai and Elsworth*, 1994; *Ouyang and Elsworth*, 1993]

$$k_0 = \frac{b_0^3}{12s}, \tag{3}$$

where b_0 is the initial fracture aperture.

[9] For the cases where bulk in situ permeability is known, the initial fracture aperture, b_0, can then be estimated from

$$b_0 = \sqrt[3]{12sk_0}, \tag{4}$$

then the permeability evolution may be evaluated as [*Liu and Elsworth*, 1997]

$$\frac{k}{k_0} = \left(1 + \frac{\Delta b}{b_0}\right)^3, \tag{5}$$

where Δb represents the change in aperture driven by any process. This allows the evolution of fracture permeability to be followed for an arbitrary evolution of fracture aperture

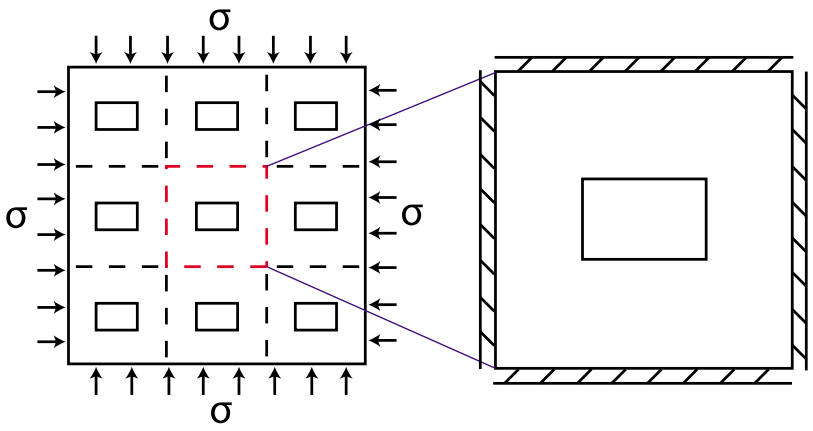

Figure 3. Schematic of the boundary condition switch. The significant difference in stiffness transforms the system from globally unconstrained to locally constrained by the development of a "stiff shell" that envelops the perimeter of an REV containing a fracture.

provided a linkage is provided with mechanisms of fracture dilation or compaction [e.g., *Elsworth and Goodman*, 1986].

2.1. Sorption-Induced Swelling Response

[10] Sorption-induced coal matrix swelling, to some extent, contributes to the reduction in permeability with increasing pore pressure, under uniaxial strain conditions [*Clarkson et al.*, 2008; *Liu and Rutqvist*, 2010; *Seidle and Huitt*, 1995; *Shi and Durucan*, 2005; *Palmer and Mansoori*, 1996; *Pan and Connell*, 2007], under displacement boundary conditions [*Liu et al.*, 2011c], and even under constant stress conditions [*Connell et al.*, 2010; *Izadi et al.*, 2011; *Mazumder and Wolf*, 2008; *Pan et al.*, 2010; *Robertson and Christiansen*, 2007; *Wang et al.*, 2011; *Zhang et al.*, 2008]. However, this permeability reduction due to sorption-induced swelling cannot be explained by the uniform free expansion concept presumed to prevail under constant stress conditions. To the contrary, free swelling of an unconstrained homogeneous medium does not change the porosity of the system [*Liu et al.*, 2011c]. The rock bridge model proposed by *Izadi et al.* [2011] utilizes constrained swelling of a lattice of repeating compartments containing a single finite fracture. This geometrically constrained swelling produces the typical response observed in unconstrained core-flooding experiments. This new work characterizes these intrinsic scaling relationships linking permeability evolution to the geometry and mechanical characteristics of the fractured medium by extension of the dual stiffness concept.

[11] We posit that the significant difference in stiffness between fracture and matrix may transform the composite system from globally unconstrained to locally constrained by the development of a "stiff shell" that envelops the perimeter of a representative elementary volume (REV) containing a fracture as displayed in Figure 3. This may be the underlying mechanism that controls permeability reduction due to sorption-induced swelling.

[12] Sorption and swelling processes have been shown to be heterogeneous in coal [*Day et al.*, 2008; *Karacan*, 2003, 2007; *Karacan and Okandan*, 2001] as apparent from quantitative X-ray CT imaging and from optical methods. In this study, coal sorption is considered to follow a Langmuir isotherm, which describes monolayer adsorption on open surfaces freely exposed to gas [*Langmuir*, 1918], and it is frequently applied to, and usually adequately models, the coal sorption isotherm [*Cui and Bustin*, 2005; *Cui et al.*, 2007; *Harpalani and Schraufnagel*, 1990; *Robertson and Christiansen*, 2007]. The Langmuir isotherm is stated as

$$\theta = \frac{\beta P}{1 + \beta P}, \tag{6}$$

where θ is the fractional coverage of the surface, P is the gas pressure or concentration, and β is a constant. We homogenize the sorption-induced volumetric strain ε_s as

$$\varepsilon_s = \varepsilon_L \frac{P_L(P - P_0)}{(P + P_L)(P_0 + P_L)}, \tag{7}$$

where P_0 is the initial pore pressure; ε_L and P_L are the Langmuir strain and Langmuir pressure, which represent the maximum swelling capacity and the pore pressure at which the measured volumetric strain is equal to $0.5\varepsilon_L$, respectively.

[13] For an idealized fracture system as illustrated in Figure 4, the volume of the coal matrix V can be written as

$$V = s^3. \tag{8}$$

Then the swelling-induced volumetric deformation can be expressed from

$$\Delta V = V\varepsilon_s. \tag{9}$$

For a three-dimensional system, this change in volume of the matrix should be equal and opposite to the induced change in volume of the fracture, which yields

$$\Delta V = s^2 \Delta b_s, \tag{10}$$

where Δb_s represents the change in fracture aperture due to sorption-induced swelling.

[14] Combining equations (8), (9), and (10), we obtain

$$\Delta b_s = \varepsilon_s s \tag{11}$$

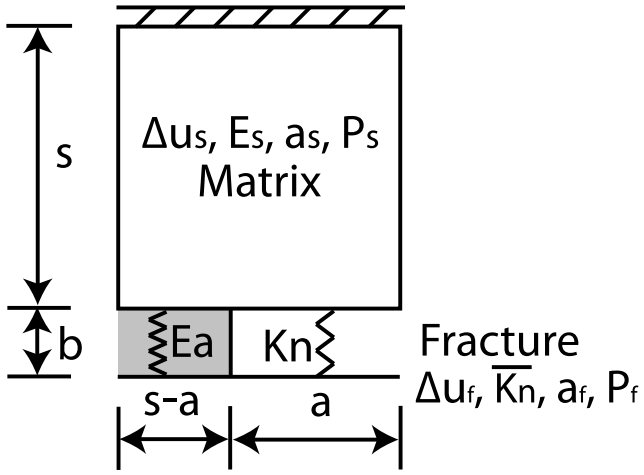

Figure 4. A simple fracture-matrix system (s) spacing, (b) aperture, and (($s - a$)/s) asperity ratio [after *Bai and Elsworth*, 1994].

and nondimensionalizing this deformation allows the normalized fracture aperture change to be defined as

$$\frac{\Delta b_s}{b_0} = \frac{\varepsilon_s s}{b_0}. \tag{12}$$

As a convention we assume that fracture opening is positive and fracture closure is negative. Therefore, permeability evolution due to sorption-induced swelling may be written as

$$\frac{k}{k_0} = \left(1 - \frac{\varepsilon_L s}{b_0}\frac{P_L(P - P_0)}{(P + P_L)(P_0 + P_L)}\right)^3. \tag{13}$$

For a fractured medium as represented above, the porosity of the system may be written as

$$\phi_0 = \frac{3b_0}{s}. \tag{14}$$

If porosity and fracture spacing are evaluated, equation (13) may take the form

$$\frac{k}{k_0} = \left(1 - \frac{3}{\phi_0}\frac{\varepsilon_L P_L(P - P_0)}{(P + P_L)(P_0 + P_L)}\right)^3, \tag{15}$$

defining the evolution of permeability as a function of initial secondary porosity, the material coefficients of the Langmuir strain and pressure, and the applied augmentation in gas pressure applied to the sample. This is the component response required to determine the influence of swelling deformations on permeability evolution.

2.2. Poromechancial Response

[15] Since the mechanism discussed above may be the fundamental mechanism to explain a reduction in permeability driven by sorption-induced swelling then the response to effective stresses should be consistent with these boundary restraints. Hence we use the same boundary condition switch of local constraint to examine the permeability enhancement due to poromechanical responses.

[16] We consider this serial geometry of matrix and fracture [*Bai and Elsworth*, 1994; *Elsworth and Bai*, 1992] with the matrix of length s and containing a single fracture. With dilation positive as defined earlier then the opening across a fracture Δu_f may be related to the change in effective stress, $\Delta\sigma'$, total stress, $\Delta\sigma$, and applied fluid pressure in the fracture, ΔP_f, the Biot coefficient for the fracture, α_f, and the stiffness of the fracture, $\overline{K_n}$ as

$$\Delta u_f = \frac{-\Delta\sigma'}{\overline{K_n}} = \frac{-\left(\Delta\sigma - \alpha_f \Delta P_f\right)}{\overline{K_n}}. \tag{16}$$

The Biot coefficient for the fracture α_f relates the change in pore pressure to the dilatation of fracture [*Biot and Willis*, 1957]. Since the fracture is compliant, in comparison to the solid constituents, α_f is set to unity. Similarly, for the solid matrix, the expansion Δu_s may be defined in terms of modulus, E_s, fracture spacing, s, Biot coefficient for the matrix, α_s, and the fluid pressure in the solid ΔP_s as

$$\Delta u_s = \frac{-s\Delta\sigma'}{E_s} = \frac{-s(\Delta\sigma - \alpha_s \Delta P_s)}{E_s}. \tag{17}$$

Since normal displacements at the periphery of the REV (Figure 3) are restricted then $\Delta u_s + \Delta u_f = 0$ and combining equations (16) and (17) yields

$$\Delta\sigma\left(\frac{s}{E_s} + \frac{1}{\overline{K_n}}\right) - \alpha_s \Delta P_s \frac{s}{E_s} - \alpha_f \Delta P_f \frac{1}{\overline{K_n}} = 0. \tag{18}$$

Then the induced total stress is defined as

$$\Delta\sigma = \frac{\alpha_s \Delta P_s \frac{s}{E_s} + \alpha_f \Delta P_f \frac{1}{\overline{K_n}}}{\frac{s}{E_s} + \frac{1}{\overline{K_n}}}. \tag{19}$$

Assuming that gas pressures have diffused uniformly throughout the REV then $\Delta P_s = \Delta P_f = \Delta P$ and this total stress may be substituted into the displacement equation (17) as

$$\Delta u_f = \Delta b = -\Delta u_s = \frac{\left(\alpha_f - \alpha_s\right)}{\left(1 + \overline{K_n} s/E_s\right)}\frac{s\Delta P}{E_s} \tag{20}$$

and finally the result recovered from the permeability relations (equation (5)) due to the poromechanical effect is

$$\frac{k}{k_0} = \left(1 + \frac{\left(\alpha_f - \alpha_s\right)}{\left(1 + \overline{K_n} s/E_s\right)}\frac{s(P - P_0)}{b_0 E_s}\right)^3. \tag{21}$$

We find that even under local displacement-controlled boundary conditions, with increasing pore pressure, and the sensible constraint that $\alpha_f > \alpha_s$ then the fracture indeed dilates for an increment of pore fluid pressure—and this in turn increases the permeability. For a uniform homogeneous medium where $\alpha_f = \alpha_s$ the steady augmentation of gas pressure results in no net change in permeability as expected for displacement controlled boundary conditions.

[17] Assuming the modulus of the fracture asperities and the normal stiffness of the void space are E_a and K_n

(Figure 4), respectively, then the average normal stiffness of the whole fracture system may be written as

$$\overline{K_n} = \frac{E_a}{b}\frac{s-a}{s} + K_n\frac{a}{s}, \tag{22}$$

where the components representing the contributions to the fracture normal stiffness from asperities and from void space are defined sequentially. This allows the fracture normal stiffness to be evaluated for an arbitrary geometry of fracture network given these controlling parameters.

2.3. System Response

[18] In this work, the matrix poromechanical deformation is controlled by the effective stress and the modulus of the matrix and is assumed to be linear. The fracture deformation is controlled by the effective stress and the fracture stiffness that is nonconstant. Thus the fracture deformation in this study is nonlinear. The matrix deformation due to sorption-induced swelling follows a Langmuir isotherm relationship with pore pressure and thus it is nonlinear. The total stress conditions we apply in this work are relatively low, at ~6 MPa. Coal samples loaded under these conditions are assumed to be within the range of elastic deformation. Therefore, the matrix and fracture deformations are treated as fully recoverable. The deformations in normal closure or opening are the predominant modes of permeability alteration. For systems under stress boundary condition, the response of the system to changes in pore pressure may be determined from consideration of the combined effects of poromechanical response and sorption-induced swelling response.

[19] In this study we focus on systems under applied stress boundary conditions as this is the most convenient way to both measure responses in the laboratory and to migrate between constraint states for prototype behavior. This is the most common boundary condition for laboratory experiments, and we can use experimental results to validate our model. So far all efforts reported in the literature have used the processes in parallel form to evaluate coal permeability evolution when using the cubic dependency, as expressed in equation (2). The nature of this equation is that the effects of poromechanical response and sorption-induced swelling on the change of fracture aperture are simultaneous. In other words, the physical processes of poromechanical response and sorption occur simultaneously. However, this may not be true for a dual permeability system. When gas is injected to a dual permeability sorbing medium, pore pressure within the medium increases via two separate processes: one that is near instantaneous in the highly permeable fracture system and one that is slow and diffusive in the low permeable matrix. The ratio of the time scales of these two processes depends on the ratio of the permeabilities within the fracture network and the matrix—and these may readily be mismatched by more than 2–3 orders of magnitude [*Wang et al.*, 2011]. This mechanism is a consequence of the partitioning of the effective stress between the fracture (that responds quickly to the perturbation) and the matrix (that responds slowly). With the observation that both poromechanical and swelling processes can alter coal permeability by orders of magnitude [*Durucan and Edwards*, 1986; *Somerton et al.*, 1975; *Wang et al.*, 2011], this is such a unique and an important feature for dual permeability dual stiffness sorbing media that it may require that the separated timing of these two effects is considered in permeability evolution models. Thus the processes in sequence/series cubic model accommodating the instantaneous poromechanical response in the fracture followed by the slow sorption-induced swelling process in the matrix can be expressed as

$$\frac{k}{k_0} = (1+A)^3(1-B)^3. \tag{23}$$

Here we evaluate both processes in parallel and processes in sequence/series cubic models with our well constrained laboratory experimental data to investigate the permeability evolution in coal. Equation (15) defines the component response required to determine the influence of swelling deformations solely on permeability evolution. And equation (21) defines the permeability relations only due to the poromechanical effect. Combining equations (15) and (21) we obtain the evolution of permeability in coal accommodating the poromechanical response and sorption-induced swelling response in the parallel mode and expressed in the format of equation (2) as

$$\frac{k}{k_0} = \left(1 + \frac{(\alpha_f - \alpha_s)}{(1+\overline{K_n}s/E_s)}\frac{s(P-P_0)}{b_0E_s} - \frac{3}{\phi_0}\frac{\varepsilon_L P_L(P-P_0)}{(P+P_L)(P_0+P_L)}\right)^3 \tag{24}$$

or in the series mode and expressed in the format of equation (23) as

$$\frac{k}{k_0} = \left(1 + \frac{(\alpha_f - \alpha_s)}{(1+\overline{K_n}s/E_s)}\frac{s(P-P_0)}{b_0E_s}\right)^3\left(1 - \frac{3}{\phi_0}\frac{\varepsilon_L P_L(P-P_0)}{(P+P_L)(P_0+P_L)}\right)^3. \tag{25}$$

Figure 5 illustrates the effects of poromechanical response and sorption-induced swelling on the evolution of permeability for sorbing media under constant total stress. The gray area on the plot is the range of the net change in permeability due to these two effects. Under constant total stress, the rate of permeability gain due to poromechanical response exponentially increases but the rate of permeability loss due to sorption-induced swelling monotonically declines following a Langmuir type pattern. Thus the role of Langmuir pressure is apparent in controlling the turnover of permeability.

2.4. Biot Coefficients and Fracture Normal Stiffness

[20] The Biot coefficient α, which controls the magnitude of the rock dilation due to an increase of the pore pressure, depends on the relative stiffness of the skeleton, K, and the solid constituents as [*Nur and Byerlee*, 1971]

$$\alpha = 1 - K/K_s, \tag{26}$$

where K_s is the bulk modulus of the solid constituents (i.e., grains). By definition, the range of variation of α is (0, 1). Relationships between aperture and effective stress acting across fractures and indexed by contact area have been previously described [*Bai and Elsworth*, 2000; *Jaeger et al.*, 2007; *Rutqvist and Stephansson*, 2003]. According to

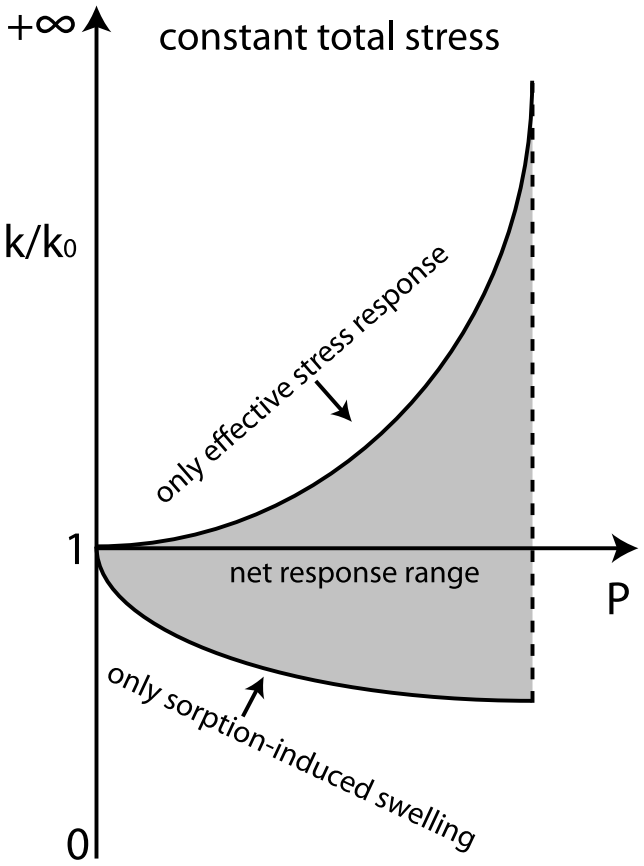

Figure 5. Illustration of permeability evolution for sorbing media under constant total stress. The gray area is the range of the net permeability evolution controlled by the competing processes of poromechanical and swelling responses.

Murdoch and Germanovich [2006], for a single fracture the Biot coefficient is the ratio of open area to the total area of the fracture surface. For a fractured medium, homogenization and upscaling will depend on the characteristics of individual fractures, as well as the fracture density and geometry of the fracture network. Thus, in our study, we postulate that the Biot coefficients for fracture and matrix are significantly different due to their distinct features. Since the equivalent stiffness of a fracture is small in comparison to that of solid grains then from equation (26) $\alpha_f \sim 1$. Typical Biot coefficients are of the order of 0.19 for marble, 0.27–0.47 for granite, and 0.64–0.85 for sandstone [*Detournay et al.*, 1989; *Elsworth and Bai*, 1992; *Hart and Wang*, 1995; *Rice and Cleary*, 1976]. Biot coefficient decreases to 0.1 in crystalline rock when the sample is loaded to a confining pressure of 100 MPa [*Schmitt and Zoback*, 1989], showing the pressure dependence. We use α_s = 0.65 as averaged from tests conducted on coal using methane [*Yangsheng et al.*, 2003].

[21] The relationship between normal stiffness of fractures and stress for rock has been studied extensively and many models have been proposed [*Bandis et al.*, 1983; *Goodman*, 1976; *Pyrak-Nolte and Morris*, 2000; *Pyrak-Nolte et al.*, 1987; *Walsh*, 1981]. For a fracture with two rough surfaces in contact, the stiffness increases as normal compressive stresses are increased – this is because more asperities come into contact. The theory shows that fracture stiffness increases linearly with increasing normal stress, and this relationship is found to hold to a good approximation in field experiments [*Walsh*, 1981; *Walsh and Grosenbaugh*, 1979]. The magnitudes of normal stiffness of rocks in the laboratory are of the order of $1–10^4$ GPa/m [*Pyrak-Nolte and Morris*, 2000; *Rutqvist et al.*, 1997]. The mechanical and hydraulic behaviors of a single fracture or fracture network in coal, however, are not well understood due to its complex structure in nature. In this study, we apply the linear relationship proposed by *Walsh and Grosenbaugh* [1979, Figure 7] as

$$\overline{K_n} = \overline{K_{n0}}\sigma'/\sigma'_0, \tag{27}$$

where $\overline{K_{n0}}$ represents the initial fracture normal stiffness at the initial effective stress, σ'_0 and σ' represents the variable effective stress. This describes the fracture normal stiffness change resulting from a change in effective normal stress.

3. Experimental Comparisons

[22] In this section, we first use the permeability model to match our own experimental data [*Wang et al.*, 2011], and then we validate this model against experimental data published in the literature [*Pini et al.*, 2009; *Robertson and Christiansen*, 2007]. The model identified in the preceding may be compared with behavior observed in a variety of flow-through experiments conducted on coal [*Wang et al.*, 2011] for different fracture geometries to define the fidelity of the proposed characterization. In these experiments, coal samples collected across the United States (Colorado, Pennsylvania, Utah, and West Virginia) are subjected to conditions of constant total stress (6 MPa), where pore pressures (He and CO_2) are increased (from 1 MPa to 5 MPa). Detailed descriptions of the experimental method and measurement procedures are given by *Wang et al.* [2011]. An intact sample with small natural embedded fractures and a similar sample but with a single thoroughgoing fracture that cleaves the sample into two unattached halves are used to evaluate the sorption-induced swelling effect on the evolution of permeability. Experiments are conducted with He and CO_2 and at room temperature. The influence of effective stress-driven changes (poromechanical response) in volume are examined with nonsorbing He as the permeant. Permeabilites to CO_2 are measured to determine the influence of adsorption and swelling on the evolution of permeability.

[23] Observations show that for the intact sample with small embedded fractures the permeability first decreases by a factor of 78% with an increase in pore pressure to 2.8 MPa (due to swelling) and then increases to a factor of 10 at a pore pressure of 4.8 MPa (due to the overriding influence of effective stress). Conversely, this turnaround in permeability from decreasing to increasing with increasing pore pressure is absent in the discretely fractured sample—the influence of the constraint of the connecting fracture bridges in limiting fracture deformation is importantly absent.

[24] We first show the comparison between model and experimental results for the sample with a longitudinal

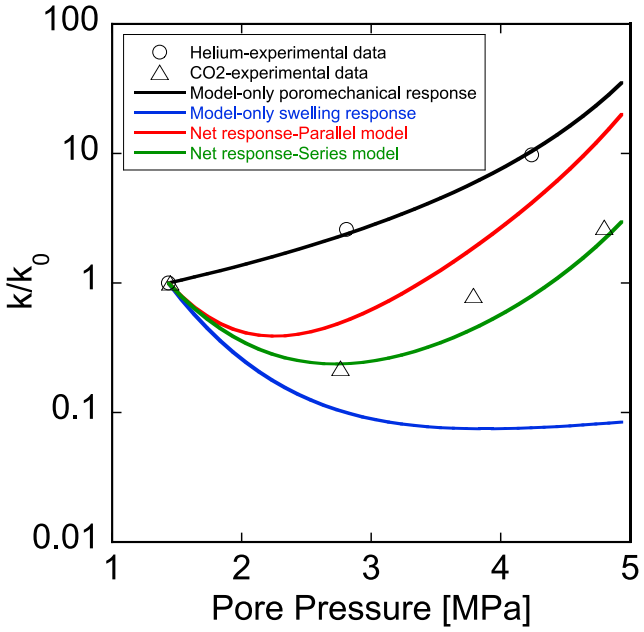

Figure 6. Comparison of permeability model results with data from a flow-through test on a sample with small natural embedded fractures. Confining stress of 6 MPa held constant and pore pressure incremented from 1.4 to 4.8 MPa. Modeled results are for the parameters defined in Table 1. Fracture stiffness is calculated from the results for helium. Initial drop in permeability to CO_2 is due to the sorption-induced swelling effect (<2.8 MPa) and later the enhancement is controlled by the poromechanical response.

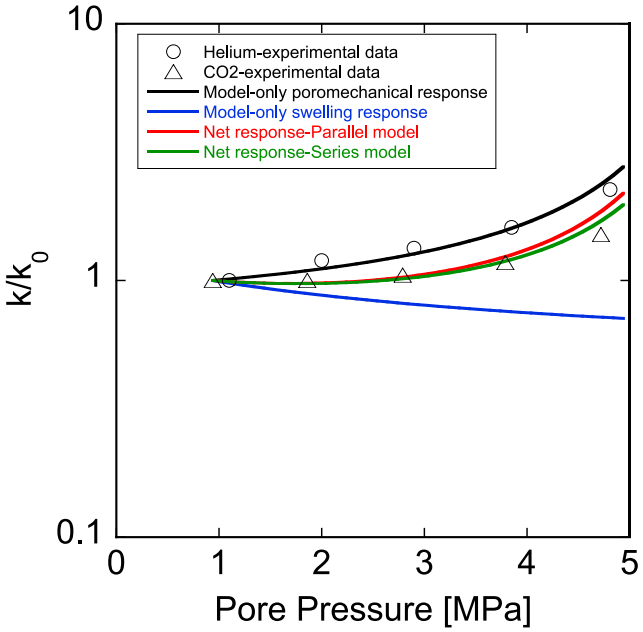

Figure 7. Comparison of permeability model results with data from a flow-through test on a sample with a longitudinal throughgoing fracture. Confining stress of 6 MPa held constant and pore pressure incremented from 0.8 to 4.8 MPa. Modeled results are for the parameters defined in Table 1. Fracture stiffness is calculated from the results for helium. The regime of decreasing permeability in the swelling regime is not observed for a fully cleaved fracture in coal absent joining rock bridges. This observation implies that the presence of bridges across fractures is a crucial component in controlling the permeability evolution with pore pressure.

throughgoing fracture. From the initial permeability of 7.2×10^{-16} m^2 we calculate the initial fracture aperture to be ~6 μm. Utilizing the permeability evolution curve for the nonadsorbing gas (He) we obtain the initial stiffness of the throughgoing fracture as ~2000 GPa/m—this is consistent with other measurements [*Pyrak-Nolte and Morris*, 2000; *Rutqvist et al.*, 1997]. We then use this calculated fracture stiffness, matrix modulus and the Langmuir sorption parameters to rematch the permeability evolution for an adsorbing gas (CO_2). For the sample with small embedded fractures, we use the fracture stiffness calculated from the discretely fracture sample and the modulus of asperities to obtain the averaged fracture stiffness for the "intact" sample, as expressed in equation (21). Then the following procedures are the same as described above. Fits with these data are completed to concurrently match the permeability evolution for both samples. These fits are shown in Figure 6 for the sample with embedded fractures and in Figure 7 for the sample with a longitudinal throughgoing fracture. The parameters utilized for the fits are identified in Table 1. The change in permeability is evaluated from equation (25). The calculated changes in permeability closely follow the observed responses. Notably, the maximum closure of the fracture is well represented by the Langmuir pressure.

[25] Figure 8 shows the results of the current model in comparison to experimental data from *Robertson and Christiansen* [2007] for subbituminous coal collected from the Anderson seam Powder River basin, Wyoming. Mechanical properties and swelling parameters are directly obtained from *Robertson and Christiansen* [2007]. As shown in Figure 8, under conditions of constant confining stress and with increasing pore pressure, permeability first drops by a factor of ~33% with an increase in pore pressure to 2.96 MPa (due to swelling), and then increases to roughly its original value at a pore pressure of 5.38 MPa (due to the overriding poromechanical effect). Fairly good matches are obtained between the model results and the laboratory data. Another attempt is made to compare the model results with the laboratory data from *Pini et al.* [2009] for bituminous coal from Monte Sinni, Italy. Coal mechanical properties, swelling parameters, and experimental data are obtained from *Pini et al.* [2009]. Permeability decreases by a factor of 27% with an increase in pore pressure to 1.76 MPa and increases to a factor of 255% at a pore pressure of 6 MPa due to the

Table 1. Magnitudes of Model Constants[a]

Sample	α_f	α_s	$\overline{K_{n0}}$ (GPa/m)	E_s (GPa)	s (m)	b_0 (μm)	ϕ (%)	P_L (MPa)	ε_L
"Intact"	1	0.65	3580	4	0.025	0.57	2	2.72	0.043
"Split"	1	0.65	2000	4	0.025	6	3	2.72	0.002

[a]"Intact" sample refers to the sample with small embedded fractures. "Split" sample represents the sample with a longitudinal throughgoing fracture.

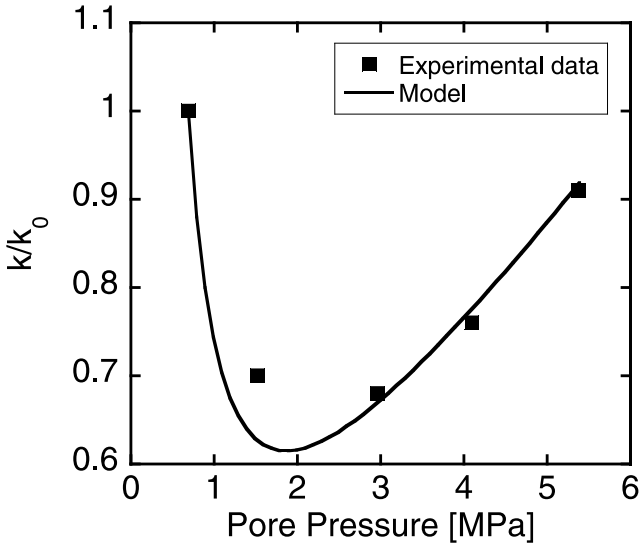

Figure 8. Comparison of model with data from *Robertson and Christiansen* [2007].

overriding poromechanical response. Figure 9 shows that the current model can predict the permeability evolution behavior reasonably well against the laboratory data. These two comparisons between model results and laboratory data suggest the fidelity of this model, at least for the data under consideration.

4. Parametric Response

[26] With the capability to replicate observed responses established in the previous, anticipated features in the response to changes in varied mechanical properties of systems (Langmuir pressure, Langmuir strain, fracture stiffness, and matrix modulus) and geometric effects of fractures and matrix (fracture spacing, fracture aperture, contact area ratio, Biot coefficients) may be straightforwardly investigated. These will reveal important features in their anticipated behavior, characteristic responses and the magnitudes of various parameters which condition this response. These behaviors are examined in the following.

[27] For the mechanical properties of the system, we evaluate the effects of Langmuir pressure, Langmuir strain, fracture stiffness, and matrix modulus. These are provided in Figure 10. Figure 10a shows that as the Langmuir pressure is increased, the amount of permeability reduction decreases. This pattern is true for the observed behavior that permeability reduction of CO_2 for coal due to swelling is larger than that of CH_4 as CO_2 has a lower Langmuir pressure than CH_4 [*Robertson and Christiansen*, 2007; *Wang et al.*, 2011]. With the same Langmuir strain, the change in Langmuir pressure alters the magnitude of the peak permeability reduction significantly but the onset of this peak in terms of pore pressure is altered only slightly. This only small change results due to the negligible influence of Langmuir pressure on the ultimate magnitude of swelling strain—it displaces the peak with respect to the absolute gas pressure. Conversely, as expected, increasing Langmuir strain increases the peak permeability reduction and also offsets the peak permeability reduction to the right as shown in Figure 10b [*Wang et al.*, 2011]. Thus in reality, since CO_2 has a smaller Langmuir pressure and larger Langmuir strain, the permeability evolution curve of CO_2 may be located directly underneath that of CH_4. By changing the same ratio of Langmuir pressure and Langmuir strain, we find that the latter has a larger effect on the permeability evolution. Thus, the permeability evolution in coal is more sensitive to the Langmuir strain.

[28] The mechanical stiffness or compliance of fractures depends primarily upon the area of contact between the two surfaces of a fracture and fluid flow through a fracture depends primarily on the smallest aperture in the flow path. The area of contact and the apertures of the void spaces adjacent to these areas of contact depend on the topographies of the two rough surfaces of the joint and on their deformation under stress [*Cook*, 1992]. Figures 10c and 10d show the effects of fracture stiffness and matrix modulus on the evolution of permeability. With the same sorption-induced swelling effects, increasing fracture stiffness will limit the deformation of the fracture and hence decrease the poromechanical effect on permeability evolution. This in turn results in the system being more sensitive to swelling and thus further decreases the net change in permeability (over the case of systems with smaller fracture stiffness). Similarly, for a system locally constrained by the development of a "stiff shell" that envelops the perimeter of an REV containing a fracture, then increasing matrix modulus prevents the contraction of the matrix and thus limits the dilation of the fracture induced by the injection of gas, as observed in Figure 10d. If we change the fracture stiffness and matrix modulus by the same ratio, then we find that fracture stiffness has a relatively larger effect on the evolution of permeability. Since equation (20) can be rewritten as

$$\frac{\Delta b}{b_0} = \frac{(\alpha_f - \alpha_s)}{(E_s + \overline{K_n} s)} \frac{s\Delta P}{b_0}, \tag{28}$$

then a comparison between equation (5) and equation (28) indicates that the effect of poromechanical response is

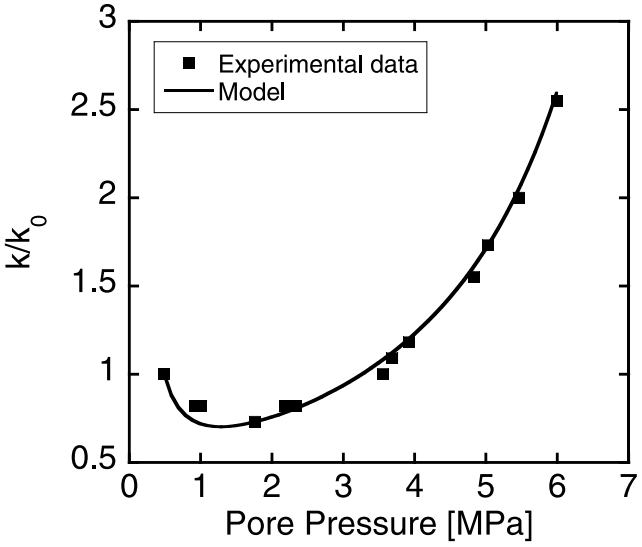

Figure 9. Comparison of model with data from *Pini et al.* [2009].

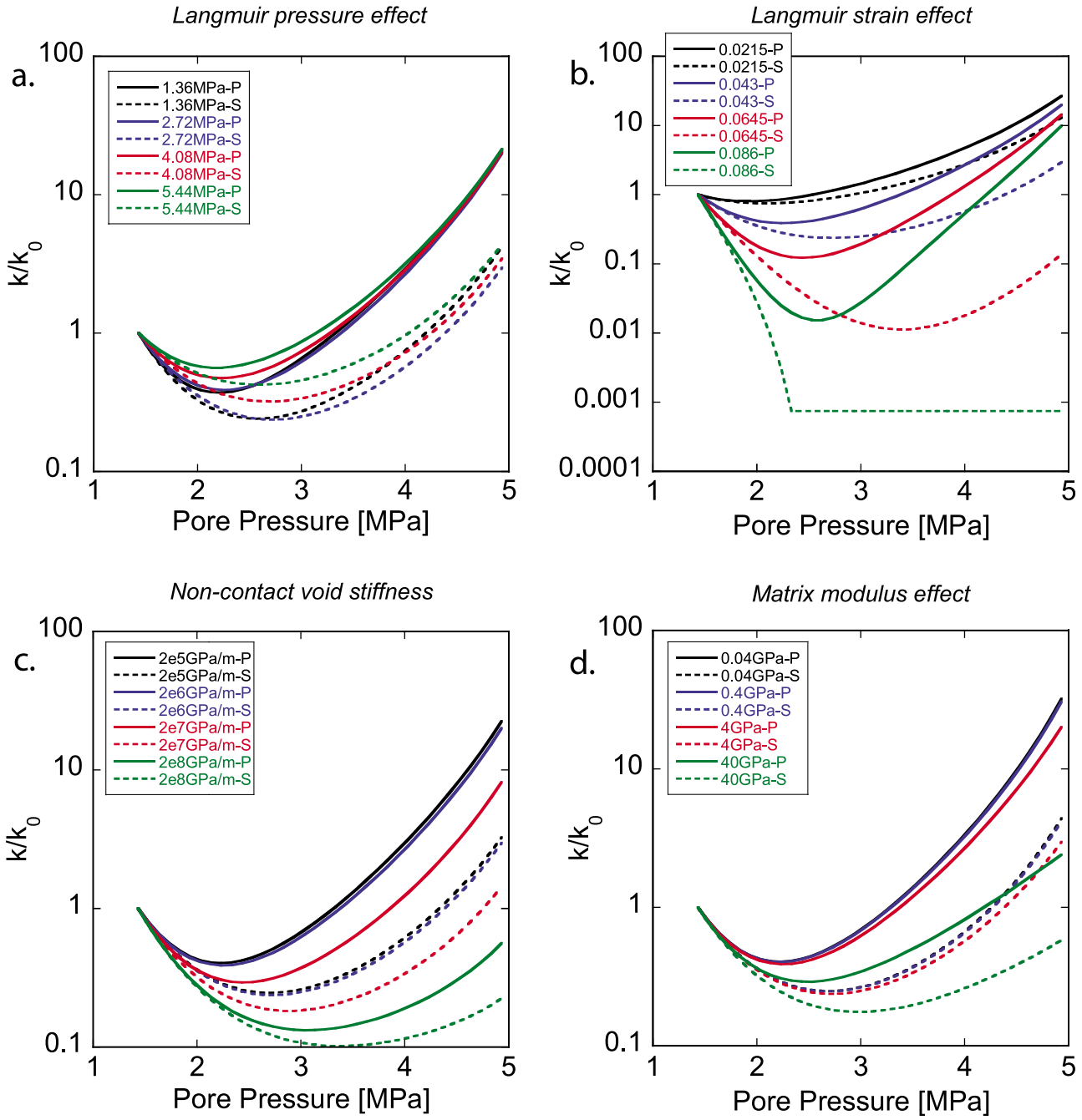

Figure 10. Parametric study of mechanical properties effects on permeability evolution. P represents parallel model results as solid lines, and S represents series model results as dashed lines. (a) Langmuir pressure effect, (b) Langmuir strain effect, (c) noncontact void stiffness effect, and (d) matrix modulus effect.

controlled by the stiffness terms "E_s" and "$\overline{K_n}s$." Permeability is little influenced when these terms are individually, or collectively, very large. For a given system, when $E_S \ll \overline{K_n}s$, which may be rare in reality, the behavior is dominated by the fracture compliance alone, as shown in Figure 10c. Similarly, there may exist a critical value of $\overline{K_n}$, as $\overline{K_n}s \ll E_S$, where the system is effectively only controlled by the properties of the matrix, as shown in Figure 10d. Therefore, there may exist critical values of fracture stiffness and matrix modulus below which permeability is not significantly dependent on the particular mechanical properties anymore.

[29] Geometric effects, including fracture spacing, fracture aperture, noncontact area ratio, and Biot coefficients for fracture and matrix, are intrinsically important as implied by equation (24) and (25). Here we vary these parameters and evaluate these effects on the evolution of permeability. Figure 11a illustrates that the smaller the fracture spacing, the larger the permeability reduction. It infers that for the

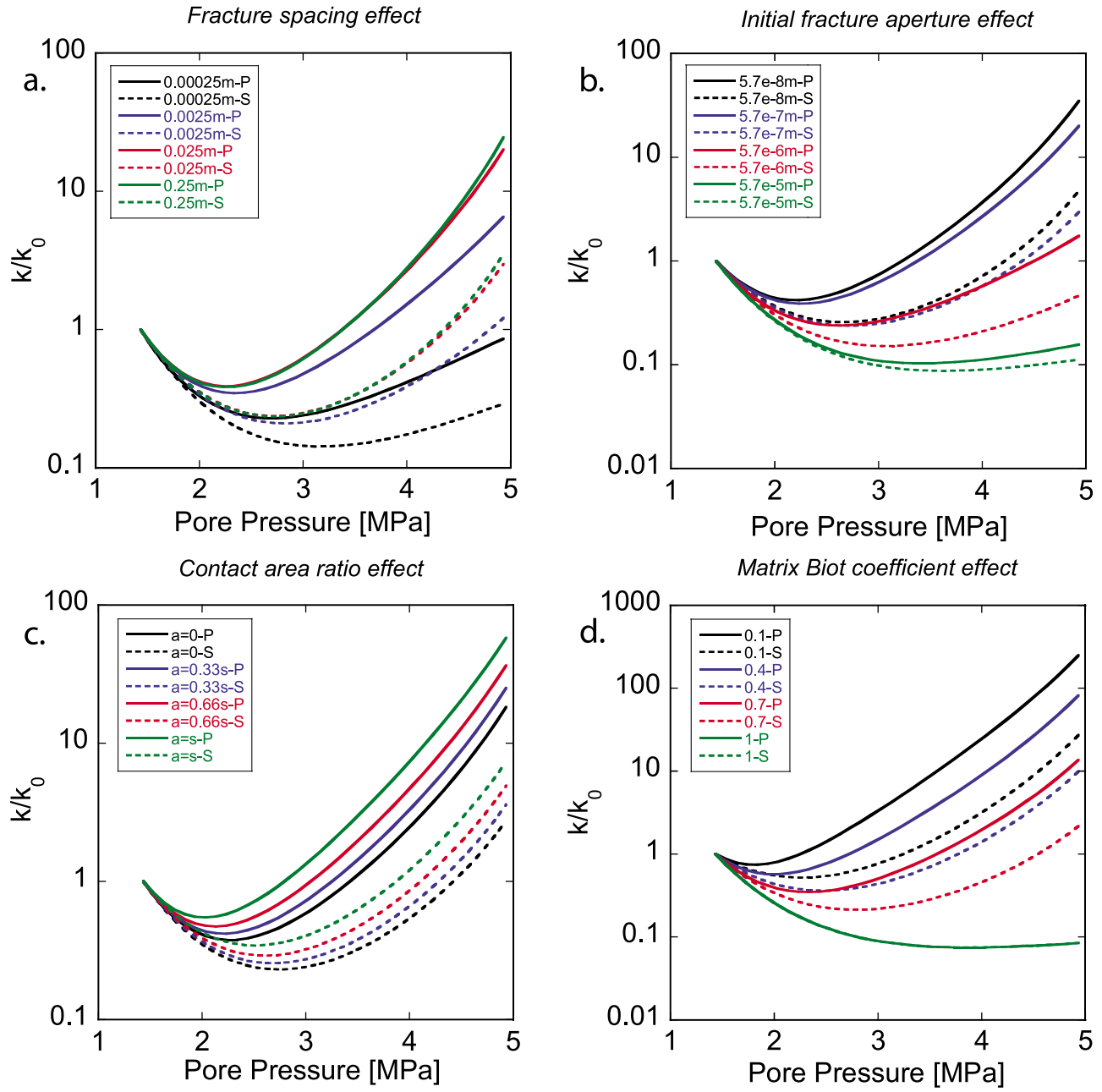

Figure 11. Parametric study of geometric effects on permeability evolution. P represents parallel model results as solid lines and S represents series model results as dashed lines. (a) Fracture spacing effect, (b) initial fracture aperature effect, (c) contact area ratio effect, and (d) matrix Biot coefficient effect.

same stress and pressure conditions, the highly fractured coal may experience a larger permeability drop compared to slightly fractured coal. Figure 11b shows the effect of the initial fracture aperture on the evolution of permeability. The poromechanical effect for coal with a smaller fracture aperture is relatively large compared with coal having a larger fracture aperture, as seen from the curves in Figure 11b. The maximum permeability drop increases with an increase in the initial fracture aperture, and the final permeability increases with a decrease in the initial fracture aperture. This observation is germane for tight organic-rich shale gas which has a narrower fracture aperture and a greater stiffness, compared with coal and suggests that both poromechanical and swelling effects may significantly influence permeability.

[30] Assuming a null initial pore pressure P_0 in the system where the reference initial permeability k_0 is defined, then the evolution of permeability in sorbing media may be rewritten as

$$\frac{k}{k_0} = \left(1 + \frac{(\alpha_f - \alpha_s)}{(1 + \overline{K_n} s/E_s)} \frac{s}{\sqrt[3]{12 k_0 s}} \frac{P_L}{E_s} \frac{P}{P_L}\right)^3 \cdot \left(1 - \frac{s}{\sqrt[3]{12 k_0 s}} \varepsilon_L \frac{P/P_L}{(P/P_L + 1)}\right)^3. \quad (29)$$

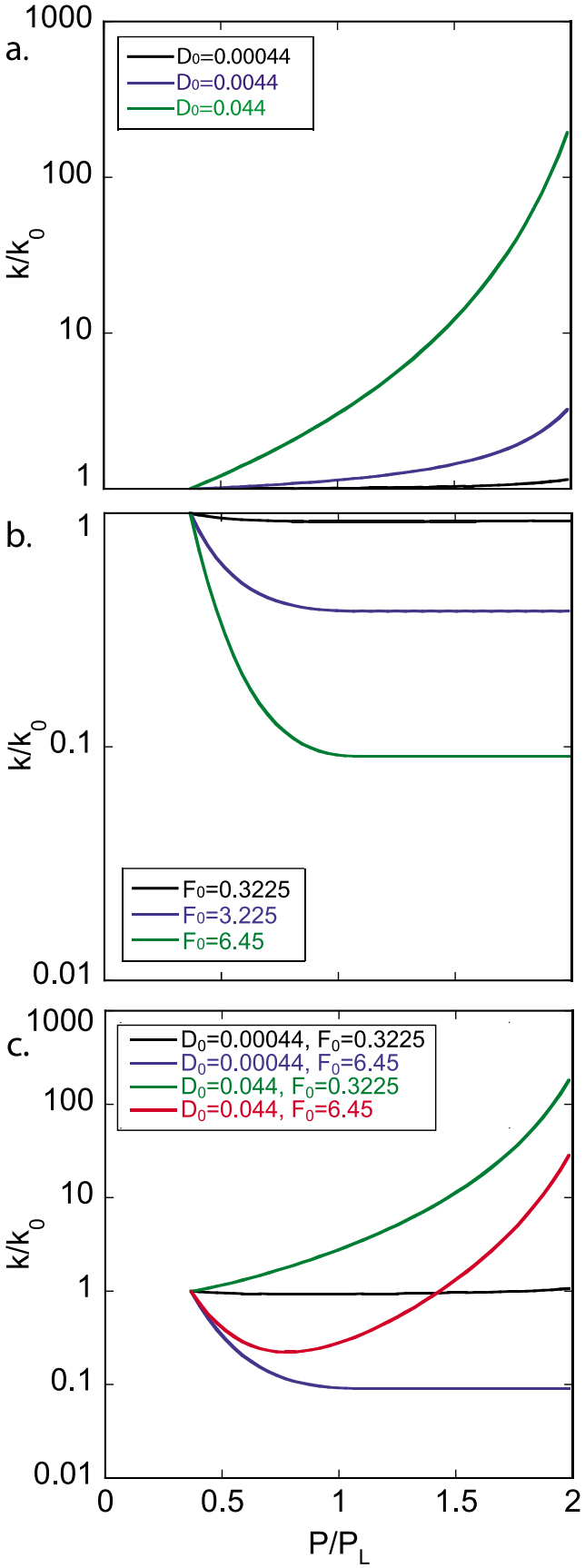

This defines the evolution of permeability for a nonsorbing fluid (where $\varepsilon_L = 0$) as a function of four dimensionless parameter groups, $\frac{(\alpha_f - \alpha_s)}{(1+\overline{K_n}s/E_s)}$, $\frac{s}{\sqrt[3]{12k_0 s}}$, $\frac{P_L}{E_s}$, and $\frac{P}{P_L}$. For a sorbing but homogenous medium where $\alpha_f = \alpha_s$, the evolution of permeability is dependent on three dimensionless parameters groups, $\frac{s}{\sqrt[3]{12k_0 s}}$, ε_L, and $\frac{P}{P_L}$, defining a total of five independent groups.

[31] For simplicity, we may rewrite equation (29) as

$$\frac{k}{k_0} = \left(1 + D\frac{P}{P_L}\right)^3 \left(1 - F\frac{P/P_L}{(P/P_L + 1)}\right)^3, \qquad (30)$$

where $D = \frac{(\alpha_f - \alpha_s)}{(1+\overline{K_n}s/E_s)} \frac{s}{\sqrt[3]{12k_0 s}} \frac{P_L}{E_s}$, and is the poromechanical response coefficient, and $F = \frac{s}{\sqrt[3]{12k_0 s}} \varepsilon_L$, and is the swelling response coefficient. The magnitudes of D and F are principally controlled by the parameter $\frac{s}{\sqrt[3]{12k_0 s}}$, which is defined by the fracture spacing and the initial permeability of a field reservoir, and are both large with a range (2000–20000). The remaining parameters $\frac{(\alpha_f - \alpha_s)}{(1+\overline{K_n}s/E_s)}$, $\frac{P_L}{E_s}$ and ε_L and are likely to be small (0.001–0.5).

[32] For systems where gas injection or extraction is involved, we investigate the permeability evolution as a function of P/P_L while varying D and F for both limiting cases and the combined effects as well. Figure 12a shows that the poromechanical effect on the evolution of permeability is large when the controlling parameter D is large for a system where swelling effect is negligible. Similarly, Figure 12b shows that the swelling effect on the evolution of permeability is large when F is large for a system in which poromechanical effects can be neglected, such as in a homogeneous system. The combined effects are illustrated in Figure 12c. When both D and F are small, the permeability remains nearly constant with increasing pore pressure. But when either D or F is large and the other is small then characteristic responses relate to the monotonic increase due to effective stresses (large D small F) or the stabilizing decline due to swelling stresses (small D and large F). Only when both D and F are large will a turnaround in permeability result as the dominant influence of swelling wanes and is replaced by dilation due to effective stresses. Thus, for systems with even low-swelling strains, such as organic-rich shales, both the poromechanical (controlled by D) and swelling effects (controlled by F) may still be large due to the low initial permeability or small fracture aperture.

Figure 12. Generalized response of permeability evolution in coal. D_0 represents the initial poromechanical response coefficient and F_0 represents the initial swelling response coefficient. (a) The poromechanical response on the evolution of permeability with different magnitudes of D_0 when the swelling effect is negligible. (b) The swelling effect on the evolution of permeability with different magnitude of F_0 when the poromechanical effect is negligible. (c) The combined effects of poromechanical and swelling responses on the evolution of permeability. When both D and F are large, a turnaround in permeability from decreasing to increasing with increasing pore pressure is expected.

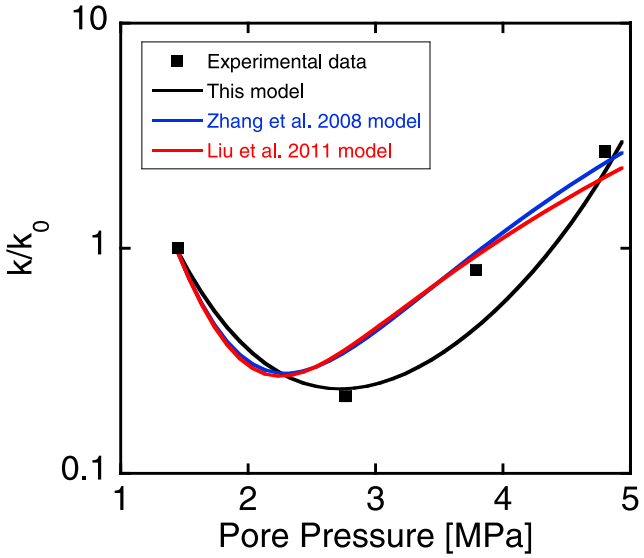

Figure 13. Comparison of the current model with the *Zhang et al.* [2008] and *Liu et al.* [2011c] models.

Hence, the characteristics of the fractures in sorbing media are extremely important in controlling the transport properties as they may control both the poromechanical and swelling responses.

5. Discussion

[33] In the previous sections we derive a mechanistic model for permeability evolution that accommodates the effects of poromechanical response and sorption-induced swelling response on the transport properties of coal. This model utilizes the concept of dual stiffness for fractured media where sorption is appropriately accommodated. Parametric studies are conducted to evaluate the sensitivity of permeability evolution to mechanical properties (Langmuir pressure, Langmuir strain, fracture stiffness, and matrix modulus) and geometric factors (fracture spacing, fracture aperture, contact area ratio, Biot coefficients). Here we extend the model to be readily applied when strain information is known alone. Then we compare the results from the current model with two previous models in the literature with the same experimental data set.

[34] Assuming that the individual fractures are distinctly soft with respect to the porous medium and $s \gg b$, then the deformation-modified permeability may be written as [*Elsworth*, 1989]

$$k = \frac{1}{12s}(b_0 + s\varepsilon)^3, \tag{31}$$

where ε is the body strain perpendicular to the fracture set with dilatational strain and fracture dilation defined as positive. The limiting condition for this expression for the system under compression must be constrained on physical grounds as

$$b_0 + s\varepsilon \geq 0. \tag{32}$$

Assuming that shear displacement and dilatation are neglected, the total displacement Δu_t, resulting from a change in stress perpendicular to the fracture sets σ, is written as

$$\Delta u_t = \Delta u_s + \Delta u_f = \left(\frac{s}{E_s} + \frac{1}{\overline{K_n}}\right)\sigma, \tag{33}$$

where Δu_s and Δu_f are the displacements of the matrix and the fracture, respectively, E_s is the elastic modulus of the matrix, and $\overline{K_n}$ is the normal stiffness of the fracture. The displacement across the fractures can be evaluated from equation (31) as

$$\Delta u_f = \varepsilon\left(\frac{\overline{K_n}}{E_s} + \frac{1}{s}\right)^{-1}. \tag{34}$$

When strains are known, the deformation-induced permeability evolution can be calculated by using

$$\frac{k}{k_0} = \left[1 - \varepsilon\left(\frac{\overline{K_n} b_0}{E_s} + \frac{b_0}{s}\right)^{-1}\right]. \tag{35}$$

Equation (35) indicates that the effect of induced strains on permeability are controlled by the dimensionless terms $\overline{K_n} b_0/E_s$ and b_0/s. Permeability is little influenced when these terms are individually, or collectively, very large.

[35] As shown in Figures 10 and 11, both the processes in parallel and the processes in sequence/series cubic permeability model forms can replicate the behavior observed in the laboratory. Again, the parallel form assumes that the poromechanical process and sorption process occur simultaneously. The series form is based on the concept that the poromechanical process is near instantaneous and sorption is a slow and diffusive process, and thus they occur sequentially. We emphasize that little is known about the relative timing between these two processes. It is worth mentioning that for the models we run at the final pore pressure of ~5 MPa, the magnitude of permeability from the parallel from is 1 order of magnitude larger than that from the series form. Apparently, one can match experimental results with either one of these two models by adjusting parameters. Our data in this study favor the series model.

[36] Figure 13 shows the results of the current model in comparison to alternative permeability models. Two models (*Zhang et al.* [2008] model and *Liu et al.* [2011c] model) are considered. The *Zhang et al.* [2008] model is a single permeability model that considers the effects of poroelasticity and sorption-induced swelling. It takes the form as

$$\frac{k}{k_0} = \left(\frac{1}{1+S}\left((1+S_0) + \frac{\alpha}{\phi_0}(S - S_0)\right)\right)^3, \tag{36}$$

$$S_0 = (p_0/K_S) - \varepsilon_L p_0/(p_0 + p_L), \tag{37}$$

$$S = \varepsilon_V + (p/K_S) - \varepsilon_S, \tag{38}$$

where ε_V is the volumetric strain.

[37] The *Liu et al.* [2011c] model is a dual permeability model that adopts the concept of modulus reduction ratio and it is expressed as

$$\frac{k}{k_0} = \frac{k_{m0}}{k_{m0}+k_{f0}}\left(1+\frac{\alpha}{\phi_{m0}}R_m\frac{\Delta\sigma-\Delta p_m}{K}\right)^3 + \frac{k_{f0}}{k_{m0}+k_{f0}}\left(1+\frac{(1-R_m)}{\phi_{f0}}(\Delta\varepsilon_V-\Delta\varepsilon_S)\right)^3, \quad (39)$$

where subscripts m and f represent matrix and fracture, respectively. R_m is the modulus reduction ratio that represents the ratio of the partitioned strain for the fracture system to the total equivalent strain.

[38] As shown in Figure 13, with the same coal properties and swelling parameters, all three models capture the key competing processes of sorption-induced swelling and poromechanical dilation and provide fairly good matches. Compared with the current model, these two previous models slightly underestimate the peak reduction in permeability. However, the two previous models are rather complicated and require numerical solution. The fundamental difference between the current model and these two previous models is that the current model explicitly takes account of the interaction between fracture and matrix. The current model does not need a numerical code to solve for response and thus is easier to implement. The limitation in the *Liu et al.* [2011c] model is that it requires knowledge of the matrix permeability, which may be difficult to measure in the laboratory and in the field.

6. Implications to Field CO_2 Sequestration and for Coalbed Methane

[39] Since the concept of CO_2 sequestration was first proposed in 1991 [*Gunter et al.*, 1997], a number of field CO_2-ECBM storage pilot projects have been undertaken around the world [*White et al.*, 2005]. However, one of the technical obstacles faced in practice is that permeability reduces during injection of CO_2 [*Levine*, 1996; *Pekot and Reeves*, 2002]. This permeability reduction was observed in field projects, including the Allison Unit pilot, located in the northern New Mexico part of the San Juan Basin, where a permeability reduction of 99% was observed in the early stage of the injection and permeability was improved in the later stage [*Pekot and Reeves*, 2002]. These phenomenon may imply that the permeability reduction in the early stage is induced by the swelling and the enhancement later is caused by the poromechanical response, which our model can closely replicate these behaviors. Similar dramatic reductions in CO_2 injectivity have also been observed in other field trials and confirmed in laboratory experiments [*Chen et al.*, 2010; *Wang et al.*, 2011]. Conversely, enhancement in permeability due to reservoir pressure depletion-induced coal matrix shrinkage has been observed in CBM projects [*Fujioka et al.*, 2010; *Palmer*, 2009; *White et al.*, 2005].

[40] We demonstrate that our model is capable of providing a physical explanation of these laboratory and field observations. Thus, our parametric analyses may provide useful information to help screen areas favorable for successful application of CO_2 sequestration and ECBM. For CO_2 sequestration, in order to have a high injectivity and to maintain it high for as long as possible, one would select a site with an adequate permeability and also where the poromechanical response can quickly override the sorption-induced swelling response, thus guaranteeing that the permeability will neither drop significantly nor for a long time. For CBM or ECBM, a reservoir with large initial permeability and with the potential to have a dominant desorption-induced shrinkage effect over poromechancial effects is preferred. Our analyses show that permeability is a complex function of pore pressure. Thus, the relationship between the initial reservoir pressure and the rebound pressure (maybe the Langmuir pressure) is of crucial importance for CBM. For injection, if $P_0 > P_L$, then the permeability would decrease initially, followed by a strong rebound during extraction. Conversely, if $P_0 < P_L$, a continuous increase in permeability would be expected with continued production [*Shi and Durucan*, 2005]. For ECBM, the relationship among Langmuir pressures and Langmuir strains for CO_2 and CH_4, and the in situ pore pressure is even more complicated and important for efficiently injecting CO_2 and enhancing methane production with the same rationale.

7. Implications to Strength and Stability of Coal Seams

[41] The swelling-induced reduction in permeability may provide a self-sealing factor to the organic-rich shale caprock for CO_2 sequestration during injection. While, for safe long-term stability after the injection period, pore gases also play an important role in instability and rupture of coal seams via their effect on strength and coal-gas interactions [*Viete and Ranjith*, 2006; *Wang et al.*, 2011]. Considering a simple Coulomb model for frictional strength defined as

$$\tau = C + \mu(\sigma - P), \quad (40)$$

where τ is shear strength, C is cohesion, and μ is the coefficient of internal friction, it is clear that the shear failure strength depends inversely on pore pressure P, which is intrinsically indexed to the fracture permeability. Faulting on preexisting faults and seismic activities may induce CO_2 desorption, increase fracture permeability as described by this model, build pore pressure within the fracture for this closed formation, and then accelerate the rupture process. The rapid desorption of the abundant adsorbed gases in coal matrix has the potential to cause explosive and energetic failure, such as the instantaneous gas outbursts in underground coal mines [*Beamish and Crosdale*, 1998].

8. Conclusions

[42] A model is developed to accommodate the effects of poromechanical response and sorption-induced swelling response on the transport properties of coal. At pressures below the Langmuir pressure, increases in pore pressures elicit a competitive response between poromechanical effects that increase permeability and sorption-induced swelling that decreases permeability. The opposite is true for reductions in pressure. Above the Langmuir pressure poromechanical effects dominate. Under constant total stress,

increasing pore pressure may initially reduce the permeability at low gas pressures when swelling dominates with the permeability recovering as the Langmuir pressure is transited and the poromechanical effect dominates. These dual effects are readily accommodated in this model. In this particular representation, the poromechanical effect is controlled by the difference in Biot coefficients for fracture and for matrix, fracture stiffness, matrix modulus, fracture spacing, and fracture aperture. And the sorption-induced swelling is controlled by the Langmuir parameters. The motivation of this analysis is to produce a representation capable of capturing the essential features of the complex processes of gas injection into sorbing media which act at multiple scales. The model is applied to observational data for different ranks of coals, and different types of gases and satisfactory agreement is obtained. Major findings are summarized as follows.

[43] 1. For homogenous porous media, neither sorption-induced swelling nor poromechanical response significantly changes the permeability with increasing pore pressure under stress-controlled boundary conditions.

[44] 2. For fractured sorbing media, however, the significant difference in stiffness between fracture and matrix transforms the composite system from globally unconstrained to locally constrained system by the development of a "stiff shell" that envelops the perimeter of an REV containing a fracture. It is this shift that causes swelling-induced permeability reduction at low (sorbing) gas pressures.

[45] 3. The inequality of the Biot coefficients within the fracture and matrix results in changes in permeability due to poromechanical effects even under locally constrained boundary conditions.

[46] 4. The contact areas of asperities which bridge across fractures have a significant role in controlling permeability evolution.

[47] 5. Our experimental data favor the processes in sequence/series permeability model.

Appendix A: Existing Permeability Models

[48] The following are the existing permeability models and associated formula.*Seidle and Huitt* [1995]

$$\frac{k}{k_0}=\left[1+\frac{\varepsilon_L}{3}\left(1+\frac{2}{\phi_0}\right)\left(\frac{P_0}{P_L+P_0}-\frac{P}{P_L+P}\right)\right]^3$$

Palmer and Mansoori [1996]

$$\frac{k}{k_0}=\left[1+\frac{c_m}{\phi_0}(P-P_0)+\frac{\varepsilon_L}{\phi_0}\left(\frac{K}{M-1}\right)\left(\frac{\beta P}{1+\beta P}-\frac{\beta P_0}{1+\beta P_0}\right)\right]^3$$

Shi and Durucan [2005]

$$\frac{k}{k_0}=\exp\left\{3C_f\left[\frac{v}{1-v}(P-P_0)+\frac{\varepsilon_L}{3}\left(\frac{E}{1-v}\right)\left(\frac{P_0}{P_L+P_0}-\frac{P}{P_L+P}\right)\right]\right\}$$

Cui and Bustin [2005]

$$\frac{k}{k_0}=\exp\left\{-\frac{3}{Kp}\left[\frac{(1+v)}{3(1-v)}(P-P_0)-\frac{2E}{9(1-v)}(\varepsilon_s-\varepsilon_{s0})\right]\right\}$$

Robertson and Christiansen [2007]

$$\frac{k}{k_0}=\exp\left\{-3C_f\frac{1-\exp[\alpha_c(P-P_0)]}{\alpha_c}+\frac{9}{\phi_0}\left[\frac{1-2v}{E}(P-P_0)-\frac{\varepsilon_L}{3}\left(\frac{P_L}{P_L+P_0}\right)\ln\left(\frac{P_L+P}{P_L+P_0}\right)\right]\right\}$$

Clarkson et al. [2008]

$$\frac{k}{k_0}=\left[1+\frac{C_m}{\phi_0}(P-P_0)+\frac{1}{\phi_0}\left(\frac{K}{M}-1\right)\Delta\varepsilon_s\right]^3$$

Zhang et al. [2008]

$$\frac{k}{k_0}=\left\{\frac{1}{1+S}[(1+S_0)\phi_0+a(S-S_0)]\right\}^3,$$

$$S=\varepsilon_V+\frac{P}{K_s}-\varepsilon_s,\quad S_0=\varepsilon_V+\frac{P_0}{K_s}-\varepsilon_{s0}$$

Liu and Rutqvist [2010]

$$\frac{k}{k_0}=\exp\left[-3C_f(\sigma-\sigma_0)\right],\quad \Delta\sigma=-\Delta P+\frac{E\left(f\Delta\varepsilon_s-\Delta\varepsilon_{fl}\right)}{1-v},$$

$$\Delta\varepsilon_{fl}=\frac{1}{2}\phi_0\left(1-e^{-C_f\Delta\sigma_f}\right)$$

Liu et al. [2011c]

$$\frac{k}{k_0}=\left[1+\frac{(1-R_m)}{\phi_0}(\Delta\varepsilon_V-\Delta\varepsilon_s)\right]^3$$

Izadi et al. [2011]

$$\frac{k}{k_0}=\left[1+\left(\frac{\varepsilon_L s^2}{lb_0}\right)\frac{P}{P+P_L}\right]^3$$

This model

$$\frac{k}{k_0}=\left(1+\frac{(a_f-a_s)}{(1+\overline{K_n}s/E_s)}\frac{s(P-P_0)}{b_0E_s}\right)^3\left(1-\frac{3}{\phi_0}\frac{\varepsilon_L P_L(P-P_0)}{(P+P_L)(P_0+P_L)}\right)^3$$

Notation

a length of void, m.
A poromechanical response on the evolution of permeability.
b fracture aperture, m.
b_0 initial fracture aperture, m.
Δb change in fracture aperture, m.
Δb_s change in fracture aperture due to sorption-induced swelling, m.
B sorption-induced swelling response on the evolution of permeability.
C cohesion, Pa.
D poromechanical response coefficient.
D_0 initial poromechanical response coefficient.
E_a asperities modulus, Pa.

E_s matrix modulus, Pa.
F swelling response coefficient.
F_0 initial swelling response coefficient.
k fracture permeability, m^2.
k_0 initial fracture permeability, m^2.
K bulk modulus of coal, Pa.
K_n stiffness of void, Pa/m.
$\overline{K_n}$ average fracture normal stiffness, Pa/m.
$\overline{K_{n0}}$ initial average fracture normal stiffness, Pa/m.
K_s bulk modulus of the solid constituents, Pa.
P pore pressure, Pa.
P_0 initial pore pressure, Pa.
P_L Langmuir pressure, Pa.
ΔP_f change in pore pressure within fracture, Pa.
ΔP_s change in pore pressure within matrix, Pa.
s fracture spacing, m.
Δu_f displacement across a fracture, m.
Δu_s displacement of matrix, m.
V volume of coal matrix, m^3.
ΔV change in volume of coal matrix, m^3.

Greek symbols

α Biot cofficient.
α_f Biot coefficient for fracture.
α_s Biot coefficient for matrix.
ϕ_0 porosity.
σ total stress, Pa.
σ' effective stress, Pa.
σ_0' initial effective stress, Pa.
$\Delta\sigma$ change in total stress, Pa.
$\Delta\sigma'$ change in effective stress, Pa.
ε body strain perpendicular to the fracture.
ε_s sorption-induced swelling strain.
ε_L Langmuir strain.
τ shear strength, Pa.
μ coefficient of internal friction.

[49] **Acknowledgments.** This work is a partial result of funding by NIOSH under contract 200-2008-25702, and the National Science Foundation under grant EAR-0842134. This support is gratefully acknowledged. We thank an Associate Editor and an anonymous reviewer for valuable suggestions that helped improve the manuscript.

References

Bai, M., and D. Elsworth (1994), Modeling of subsidence and stress-dependent hydraulic conductivity for intact and fractured porous media, *Rock Mech. Rock Eng.*, *27*(4), 209–234, doi:10.1007/BF01020200.

Bai, M., and D. Elsworth (2000), *Coupled Processes in Subsurface Deformation, Flow, and Transport*, 336 pp., Am. Soc. of Civ. Eng., Reston, Va.

Bandis, S. C., A. C. Lumsden, and N. R. Barton (1983), Fundamentals of rock joint deformation, *Int. J. Mech. Min. Sci. Geomech. Abstr.*, *20*(6), 249–268, doi:10.1016/0148-9062(83)90595-8.

Beamish, B. B., and P. J. Crosdale (1998), Instantaneous outbursts in underground coal mines: An overview and association with coal type, *Int. J. Coal Geol.*, *35*(1–4), 27–55, doi:10.1016/S0166-5162(97)00036-0.

Biot, M. A., and D. G. Willis (1957), The elastic coefficients of the theory of consolidation, *J. Appl. Mech.*, *24*, 594–601.

Chen, Z., J. Liu, D. Elsworth, L. D. Connell, and Z. Pan (2010), Impact of CO_2 injection and differential deformation on CO_2 injectivity under in situ stress conditions, *Int. J. Coal Geol.*, *81*(2), 97–108, doi:10.1016/j.coal.2009.11.009.

Chen, Z., Z. Pan, J. Liu, L. D. Connell, and D. Elsworth (2011), Effect of the effective stress coefficient and sorption-induced strain on the evolution of coal permeability: Experimental observations, *Int. J. Greenh. Gas Control*, *5*(5), 1284–1293, doi:10.1016/j.ijggc.2011.07.005.

Clarkson, C., Z. Pan, I. Palmer, and S. Harpalani (2008), Predicting sorption induced strain and permeability increase with depletion for CBM reservoirs, paper presented at Annual Technical Conference and Exhibition, Soc. of Pet. Eng., Denver, Colo., 21–24 Sept.

Connell, L. D., M. Lu, and Z. Pan (2010), An analytical coal permeability model for tri-axial strain and stress conditions, *Int. J. Coal Geol.*, *84*(2), 103–114, doi:10.1016/j.coal.2010.08.011.

Cook, N. G. W. (1992), Natural joints in rock: Mechanical, hydraulic and seismic behaviour and properties under normal stress, *Int. J. Mech. Min. Sci. Geomech. Abstr.*, *29*(3), 198–223, doi:10.1016/0148-9062(92)93656-5.

Cui, X. J., and R. M. Bustin (2005), Volumetric strain associated with methane desorption and its impact on coalbed gas production from deep coal seams, *AAPG Bull.*, *89*(9), 1181–1202, doi:10.1306/05110504114.

Cui, X., R. M. Bustin, and L. Chikatamarla (2007), Adsorption-induced coal swelling and stress: Implications for methane production and acid gas sequestration into coal seams, *J. Geophys. Res.*, *112*, B10202, doi:10.1029/2004JB003482.

Day, S., R. Fry, and R. Sakurovs (2008), Swelling of Australian coals in supercritical CO_2, *Int. J. Coal Geol.*, *74*(1), 41–52, doi:10.1016/j.coal.2007.09.006.

Detournay, E., A. H. D. Cheng, J. C. Roegiers, and J. D. McLennan (1989), Poroelasticity considerations in in situ stress determination by hydraulic fracturing, *Int. J. Mech. Min. Sci. Geomech. Abstr.*, *26*(6), 507–513, doi:10.1016/0148-9062(89)91428-9.

Durucan, S., and J. S. Edwards (1986), The effects of stress and fracturing on permeability of coal, *Min. Sci. Technol.*, *3*(3), 205–216, doi:10.1016/S0167-9031(86)90357-9.

Elsworth, D. (1989), Thermal permeability enhancement of blocky rocks: One-dimensional flows, *Int. J. Mech. Min. Sci. Geomech. Abstr.*, *26*(3–4), 329–339, doi:10.1016/0148-9062(89)91981-5.

Elsworth, D., and M. Bai (1992), Flow-deformation response of dual porosity media, *J. Geotech. Eng.*, *118*(1), 107–124, doi:10.1061/(ASCE)0733-9410(1992)118:1(107).

Elsworth, D., and R. E. Goodman (1986), Characterization of rock fissure hydraulic conductivity using idealized wall roughness profiles, *Int. J. Mech. Min. Sci. Geomech. Abstr.*, *23*(3), 233–243, doi:10.1016/0148-9062(86)90969-1.

Fujioka, M., S. Yamaguchi, and M. Nako (2010), CO_2-ECBM field tests in the Ishikari coal Basin of Japan, *Int. J. Coal Geol.*, *82*(3–4), 287–298, doi:10.1016/j.coal.2010.01.004.

Gierhart, R., C. Clarkson, and J. Seidle (2007), Spatial variation of San Juan basin fruitland coalbed methane pressure dependent permeability: Magnitude and functional form, paper presented at International Petroleum Technology Conference, China Nat. Pet. Corp., Dubai, 4–6 Dec.

Goodman, R. E. (1976), *Methods of Geological Engineering in Discontinuous Rocks*, 472 pp., West, New York.

Gunter, W. D., T. Gentzis, B. A. Rottenfusser, and R. J. H. Richardson (1997), Deep coalbed methane in Alberta, Canada: A fuel resource with the potential of zero greenhouse gas emissions, *Energy Convers. Manage.*, *38*, Suppl. 1, S217–S222, doi:10.1016/S0196-8904(96)00272-5.

Harpalani, S., and G. Chen (1997), Influence of gas production induced volumetric strain on permeability of coal, *Geotech. Geol. Eng.*, *15*(4), 303–325, doi:10.1007/BF00880711.

Harpalani, S., and R. A. Schraufnagel (1990), Shrinkage of coal matrix with release of gas and its impact on permeability of coal, *Fuel*, *69*(5), 551–556, doi:10.1016/0016-2361(90)90137-F.

Hart, D. J., and H. F. Wang (1995), Laboratory measurements of a complete set of poroelastic moduli for Berea sandstone and Indiana limestone, *J. Geophys. Res.*, *100*(B9), 17,741–17,751.

Izadi, G., S. Wang, D. Elsworth, J. Liu, Y. Wu, and D. Pone (2011), Permeability evolution of fluid-infiltrated coal containing discrete fractures, *Int. J. Coal Geol.*, *85*(2), 202–211, doi:10.1016/j.coal.2010.10.006.

Jaeger, J. C., et al. (2007), *Fundamentals of Rock Mechanics*, 4th ed., 475 pp., Blackwell, Malden, Mass.

Karacan, C. O. (2003), Heterogeneous sorption and swelling in a confined and stressed coal during CO_2 injection, *Energy Fuels*, *17*(6), 1595–1608, doi:10.1021/ef0301349.

Karacan, C. O. (2007), Swelling-induced volumetric strains internal to a stressed coal associated with CO_2 sorption, *Int. J. Coal Geol.*, *72*(3–4), 209–220, doi:10.1016/j.coal.2007.01.003.

Karacan, C. O., and E. Okandan (2001), Adsorption and gas transport in coal microstructure: Investigation and evaluation by quantitative X-ray CT imaging, *Fuel*, *80*(4), 509–520, doi:10.1016/S0016-2361(00)00112-5.

Langmuir, I. (1918), The adsorption of gases on plane surfaces of glass, mica, and platinum, *J. Am. Chem. Soc.*, *40*, 1361–1403, doi:10.1021/ja02242a004.

Levine, J. (1996), Model study of the influence of matrix shrinkage on absolute permeability of coal bed reservoirs, in *Coalbed Methane and*

Coal Geology, *Geol. Soc. Spec. Publ.*, vol. 109, edited by R. A. Gayer and I. Harris, 197–212.

Liu, H.-H., and J. Rutqvist (2010), A new coal-permeability model: Internal swelling stress and fracture-matrix interaction, *Transp. Porous Media*, *82*(1), 157–171, doi:10.1007/s11242-009-9442-x.

Liu, J., and D. Elsworth (1997), Three-dimensional effects of hydraulic conductivity enhancement and desaturation around mined panels, *Int. J. Rock Mech. Min. Sci.*, *34*(8), 1139–1152, doi:10.1016/S1365-1609(97)80067-6.

Liu, J., J. Wang, Z. Chen, S. Wang, D. Elsworth, and Y. Jiang (2011a), Impact of transition from local swelling to macro swelling on the evolution of coal permeability, *Int. J. Coal Geol.*, *88*(1), 31–40, doi:10.1016/j.coal.2011.07.008.

Liu, J., Z. Chen, D. Elsworth, H. Qu, and D. Chen (2011b), Interactions of multiple processes during CBM extraction: A critical review, *Int. J. Coal Geol.*, *87*(3–4), 175–189, doi:10.1016/j.coal.2011.06.004.

Liu, J., Z. Chen, D. Elsworth, X. Miao, and X. Mao (2011c), Evolution of coal permeability from stress-controlled to displacement-controlled swelling conditions, *Fuel*, *90*(10), 2987–2997, doi:10.1016/j.fuel.2011.04.032.

Mazumder, S., and K. H. Wolf (2008), Differential swelling and permeability change of coal in response to CO_2 injection for ECBM, *Int. J. Coal Geol.*, *74*(2), 123–138, doi:10.1016/j.coal.2007.11.001.

Murdoch, L. C., and L. N. Germanovich (2006), Analysis of a deformable fracture in permeable material, *Int. J. Numer. Anal. Methods Geomech.*, *30*(6), 529–561, doi:10.1002/nag.492.

Nur, A., and J. D. Byerlee (1971), Exact effective stress law for elastic deformation of rock with fluids, *J. Geophys. Res.*, *76*(26), 6414–6419, doi:10.1029/JB076i026p06414.

Ouyang, Z., and D. Elsworth (1993), Evaluation of groundwater flow into mined panels, *Int. J. Mech. Min. Sci. Geomech. Abstr.*, *30*(2), 71–79, doi:10.1016/0148-9062(93)90701-E.

Palmer, I. (2009), Permeability changes in coal: Analytical modeling, *Int. J. Coal Geol.*, *77*(1–2), 119–126, doi:10.1016/j.coal.2008.09.006.

Palmer, I., and J. Mansoori (1996), How permeability depends on stress and pore pressure in coalbeds: A new model, paper presented at Annual Technical Conference and Exhibition, Soc. of Pet. Engineer, Denver, Colo., 6–9 Oct.

Palmer, D., J. C. Cameron, and Z. A. Moschovidis (2006), Permeability changes affect CBM production predictions, *Oil Gas J.*, *104*(28), 43–50.

Pan, Z., and L. D. Connell (2007), A theoretical model for gas adsorption-induced coal swelling, *Int. J. Coal Geol.*, *69*(4), 243–252, doi:10.1016/j.coal.2006.04.006.

Pan, Z., and L. D. Connell (2012), Modelling permeability for coal reservoirs: A review of analytical models and testing data, *Int. J. Coal Geol.*, *92*(0), 1–44, doi:10.1016/j.coal.2011.12.009.

Pan, Z., L. D. Connell, and M. Camilleri (2010), Laboratory characterization of coal reservoir permeability for primary and enhanced coalbed methane recovery, *Int. J. Coal Geol.*, *82*(3–4), 252–261, doi:10.1016/j.coal.2009.10.019.

Pekot, L. J., and S. R. Reeves (2002), Modeling the effects of matrix shrinkage and differential swelling on coalbed methane recovery and carbon sequestration, *Rep. DE-FC26-00NT40924*, U.S. Dep. of Energy, Houston, Tex.

Piggott, A. R., and D. Elsworth (1993), Laboratory assessment of the equivalent apertures of a rock fracture, *Geophys. Res. Lett.*, *20*(13), 1387–1390, doi:10.1029/93GL01384.

Pini, R., S. Ottiger, L. Burlini, G. Storti, and M. Mazzotti (2009), Role of adsorption and swelling on the dynamics of gas injection in coal, *J. Geophys. Res.*, *114*, B04203, doi:10.1029/2008JB005961.

Pyrak-Nolte, L. J., and J. P. Morris (2000), Single fractures under normal stress: The relation between fracture specific stiffness and fluid flow, *Int. J. Rock Mech. Min. Sci.*, *37*(1–2), 245–262, doi:10.1016/S1365-1609(99)00104-5.

Pyrak-Nolte, L. J., L. R. Myer, N. G. W. Cook, and P. A. Witherspoon (1987), Hydraulic and mechanical properties of natural fractures in low permeability rock, in *Proceedings of the Sixth International Congress on Rock Mechanics, Montreal, Canada*, pp. 225–231, Balkema, Rotterdam, Netherlands.

Rice, J. R., and M. P. Cleary (1976), Some basic stress diffusion solutions for fluid-saturated elastic porous media with compressible constituents, *Rev. Geophys.*, *14*(2), 227–241, doi:10.1029/RG014i002p00227.

Robertson, E. P., and R. L. Christiansen (2007), Modeling laboratory permeability in coal using sorption-induced-strain data, *SPE Reservoir Eval. Eng.*, *10*(3), 260–269, doi:10.2118/97068-PA.

Rutqvist, J., and O. Stephansson (2003), The role of hydromechanical coupling in fractured rock engineering, *Hydrogeol. J.*, *11*(1), 7–40, doi:10.1007/s10040-002-0241-5.

Rutqvist, J., O. Stephansson, and C. F. Tsang (1997), Hydraulic field measurements of incompletely closed fractures in granite, *Int. J. Rock Mech. Min. Sci. Geomech. Abst.*, *34*(3–4), 411, doi:10.1016/S0148-9062(97)00237.4.

Schmitt, D. R., and M. D. Zoback (1989), Poroelastic effects in the determination of the maximum horizontal principal stress in hydraulic fracturing tests—A proposed breakdown equation employing a modified effective stress relation for tensile failure, *Int. J. Rock Mech. Min. Sci. Geomech. Abst.*, *26*(6), 499–506, doi:10.1016/0148-9062(89)91427-7.

Seidle, J. P., and L. G. Huitt (1995), Experimental measurements of coal matrix shrinkage due to gas desorption and implications for cleat permeability increases, paper presented at International Meeting on Petroleum Engineering, Soc. of Pet. Eng., Beijing, 14–17 Nov.

Shi, J. Q., and S. Durucan (2005), A model for changes in coalbed permeability during primary and enhanced methane recovery, *SPE Reservoir Eval. Eng.*, *8*(4), 291–299, doi:10.2118/87230-PA.

Siriwardane, H., I. Haljasmaa, R. McLendon, G. Irdi, Y. Soong, and G. Bromhal (2009), Influence of carbon dioxide on coal permeability determined by pressure transient methods, *Int. J. Coal Geol.*, *77*(1–2), 109–118, doi:10.1016/j.coal.2008.08.006.

Somerton, W. H., I. M. Soylemezoglu, and R. C. Dudley (1975), Effect of stress on permeability of coal, *Int. J. Mech. Min. Sci. Geomech. Abstr.*, *12*(5–6), 129–145, doi:10.1016/0148-9062(75)91244-9.

Viete, D. R., and P. G. Ranjith (2006), The effect of CO_2 on the geomechanical and permeability behaviour of brown coal: Implications for coal seam CO_2 sequestration, *Int. J. Coal Geol.*, *66*(3), 204–216, doi:10.1016/j.coal.2005.09.002.

Walsh, J. B. (1981), Effect of pore pressure and confining pressure on fracture permeability, *Int. J. Mech. Min. Sci. Geomech. Abstr.*, *18*(5), 429–435, doi:10.1016/0148-9062(81)90006-1.

Walsh, J. B., and M. A. Grosenbaugh (1979), A new model for analyzing the effect of fractures on compressibility, *J. Geophys. Res.*, *84*(B7), 3532–3536, doi:10.1029/JB084iB07p03532.

Wang, S., D. Elsworth, and J. Liu (2011), Permeability evolution in fractured coal: The roles of fracture geometry and water-content, *Int. J. Coal Geol.*, *87*(1), 13–25, doi:10.1016/j.coal.2011.04.009.

Warren, J. E., and P. J. Root (1963), The behavior of naturally fractured reservoirs, *Soc. Pet. Eng. J.*, *3*(3), 245–255.

White, C. M., et al. (2005), Sequestration of carbon dioxide in coal with enhanced coalbed methane recovery: A review, *Energy Fuels*, *19*(3), 659–724, doi:10.1021/ef040047w.

Witherspoon, P. A., J. S. Y. Wang, K. Iwai, and J. E. Gale (1980), Validity of cubic law for fluid flow in a deformable rock fracture, *Water Resour. Res.*, *16*(6), 1016–1024, doi:10.1029/WR016i006p01016.

Yangsheng, Z., H. Yaoqing, W. Jingping, and Y. Dong (2003), The experimental Approach to effective stress law of coal mass by effect of methane, *Transp. Porous Media*, *53*(3), 235–244, doi:10.1023/A:1025080525725.

Zhang, H., J. Liu, and D. Elsworth (2008), How sorption-induced matrix deformation affects gas flow in coal seams: A new FE model, *Int. J. Rock Mech. Min. Sci.*, *45*(8), 1226–1236, doi:10.1016/j.ijrmms.2007.11.007.

Zimmerman, R. W., and G. S. Bodvarsson (1996), Hydraulic conductivity of rock fractures, *Transp. Porous Media*, *23*(1), 1–30, doi:10.1007/BF00145263.

Zimmerman, R. W., D.-W. Chen, and N. G. W. Cook (1992), The effect of contact area on the permeability of fractures, *J. Hydrol.*, *139*(1–4), 79–96, doi:10.1016/0022-1694(92)90196-3.